3D Finite Element Modelling of ICRH in WEST

B. Ljungberg[1], P. Vallejos[1], T. Johnson[1], R. Ragona[2]

[1]*Dept. of Fusion Plasma Physics, KTH Royal Institute of Technology, Stockholm, Sweden*
[2]*Laboratory for Plasma Physics, LPP-ERK/KMS, Brussels, Belgium*

Abstract

The Ion Cyclotron Resonance Heating (ICRH) antenna in WEST has been modelled with the finite element method in 3D. A detailed geometry was used along with a hot plasma model in the plasma region. The convergence of the total absorbed power and the electron power partition was studied by varying different mesh parameters. To obtain a better resolved solution and a wave field without reflections, it is estimated that 1 TB of RAM is required. The coupled power spectrum was also studied using a two-dimensional Fourier decomposition of the electromagnetic fields.

Introduction

Ion Cyclotron Resonance Heating (ICRH) has been a successful auxiliary heating method, and is widely used in tokamaks [1]. To understand the physics and investigate the performance of ICRH, it is important to model various heating scenarios. For this purpose, there are several codes using Fourier spectral methods, the finite element method (FEM) or a combination thereof. Some examples are FEMIC, EVE, TORIC and LION [2–5]. These codes use Fourier decomposition in the toroidal direction and solve the wave equation on a poloidal cross section. This makes it difficult to accurately predict the power coupling from the antenna to the plasma. Therefore, it is of interest to develop codes that can take the 3D geometrical effects into account. Such attempts have been made, for example the codes HIS-TORIC and LEMan [6, 7]. However, it may be worthwhile to investigate whether it is reasonable to model ICRH in 3D using the FEM. Therefore, the main objectives of this work is to 1) investigate the feasibility of 3D simulations in WEST using the FEMIC code by studying the convergence of total absorbed power and the electron partition of the absorbed power, and 2) study the poloidal and toroidal spectra of the power coupled from the antenna to the plasma.

The Dielectric Tensor

The dielectric tensor used in this work is the dielectric tensor for a hot bi-Maxwellian plasma. A quasi-homogeneous approximation, that is suitable for FEM, is used [8]. To evaluate the finite Larmor radius (FLR) effects in the dielectric tensor, the dispersion relation for the fast magnetosonic wave is used as in [2]. Since an algebraic tensor is used, the tensor must be evaluated for a single toroidal mode number n_ϕ, even though a spectrum of n_ϕ is expected from the antenna. The chosen mode number was $n_\phi = 42$, since it is one of the dominant mode numbers. The full toroidal spectrum could be resolved using an iterative scheme as proposed in [9]. The antenna frequency f was chosen to be $56.0\,\mathrm{MHz}$, and the on-axis toroidal magnetic field was set to $3.7\,\mathrm{T}$ in order to place the hydrogen resonance near the magnetic axis.

Model and Convergence

The tokamak was modelled as a 36° sweep of the WEST cross section. The antenna was modelled as four straps, each with tunable phase and powered by a port delivering $1\,\mathrm{W}$. The Scrape-Off Layer (SOL) in front of the plasma was meshed with a free tetrahedral mesh, while the plasma domain as well as the rest of the SOL was meshed by a free triangular mesh which was swept along the toroidal direction. The pedestal on the plasma boundary was resolved with a boundary layer mesh on both the plasma side as well as on the SOL side.

A deuterium plasma with hydrogen minority (4%) was used. The on-axis temperature (all species) was set high ($12\,\mathrm{keV}$) in order to achieve higher single pass damping, and the on-axis electron density was chosen to be $4 \times 10^{19}\,\mathrm{m}^{-3}$.

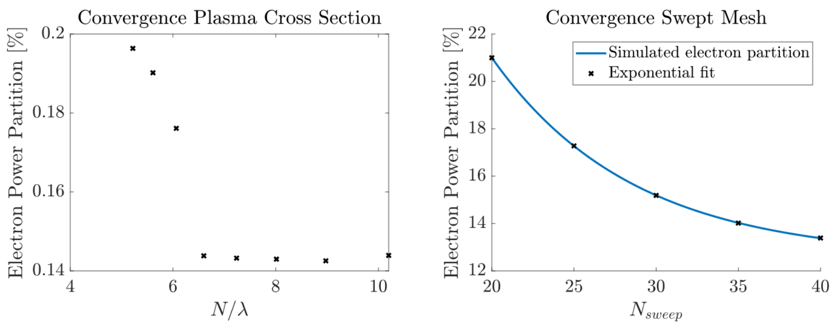

Figure 1: Convergence of the electron power partition sweeping over mesh elements per wave length in the plasma cross section (left) and the number of mesh elements in the toroidal direction (right).

To study how well the model was meshed, a convergence study was performed by computing the total absorbed power and the electron power partition for varying mesh parameters. In this paper we present only the electron power partition, as the total absorbed power varied less when changing the mesh size. Both quantities were insensitive to variations of the mesh size in the SOL. This is likely due to the geometry limiting the mesh size in front of the antenna, where the SOL resolution is most important. Increasing the overall mesh size in the SOL does not increase the size of the elements in this particular region. However, using a plasma model in the SOL may require better resolution due to mode conversion outside the antenna region.

In the plasma region, electron power partition was very sensitive to the mesh size once it was over a threshold value (see Fig. 1). Here, this threshold value is around 6 mesh elements per wavelength. It can also be seen in Fig. 1 that the convergence can be improved by increasing the number of mesh elements in the toroidal sweep, i.e. reducing the anisotropy of the mesh.

The resulting electric field and absorption density can be seen in Fig. 2. There seems to be a standing wave pattern in both the electric field and the absorption, which probably arises due to reflections on the boundaries where the tokamak has been truncated. This can then be avoided by modelling a larger sector of the machine. However, the number of degrees of freedom increases drastically with the size of the model. Modelling 70° of the tokamak with an

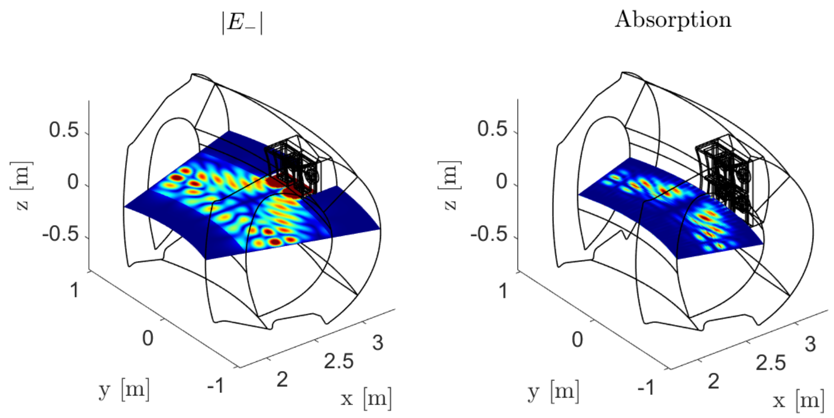

Figure 2: Right-hand polarized component of the electric field (left) and absorption density (right). The simulation was run with a plasma cross section mesh size of $0.034\,\mathrm{m}$ and $N_{sweep} = 29$.

appropriate mesh would require approximately 1 TB of RAM. This should reduce the standing wave pattern, as well as allow for a plasma model in the SOL. The model in this work has been solved using 210 GB of RAM.

Coupled Power

By Fourier decomposing the electromagnetic fields, it is possible to find an expression for the Poynting vector per mode, which then can be integrated to obtain the coupled power per mode. By choosing a suitable coordinate system, the Jacobian of this integral can be made constant, ensuring orthogonality between the different Fourier modes. This coordinate system, here called the normal-tangential coordinate system, is denoted (n, t, ϕ), where the coordinate n is the inward normal of the flux surface, t is a poloidal coordinate defined on $[0, 2\pi)$ and ϕ is the toroidal coordinate. The coupled power per mode can then be expressed as

$$P = \sum_{mn} P_{mn}, \qquad P_{mn} \equiv \frac{A}{2\mu_0} \operatorname{Re}\left\{E^{\alpha}_{mn} B^{\beta *}_{mn}\right\} \hat{\boldsymbol{e}}_n \cdot \left(\hat{\boldsymbol{e}}_\alpha \times \hat{\boldsymbol{e}}_\beta\right), \tag{1}$$

where A is the area of the separatrix, α and β denote the different vector components in the tangential-normal coordinate system, m and n are the poloidal and toroidal mode numbers, respectively. E_{mn} and B_{mn} are the Fourier components of the electric and magnetic fields, respectively. The electric and magnetic fields are Fourier decomposed in the (n, t, ϕ) coordinate system on a surface outside the separatrix. The surface was chosen not to be a flux surface to ensure Fourier decomposition on a closed surface. Instead a surface with the same shape as the separatrix was chosen, albeit enlarged by a few percent. By summing over m or n it is possible to obtain the toroidal and poloidal power spectra, respectively. P_{mn} and the toroidal power spectrum P_n are shown in Fig. 3. It can be seen in the two-dimensional power spectrum that there is an asymmetry about $m = 0, n = 0$. This asymmetry arises due to the gyrotropy of the plasma. Reversing the magnetic field or changing the sign of n when evaluating the dielectric tensor would mirror the asymmetry about $n = 0$.

It should be noted that the toroidal power spectrum changes depending on the distance to

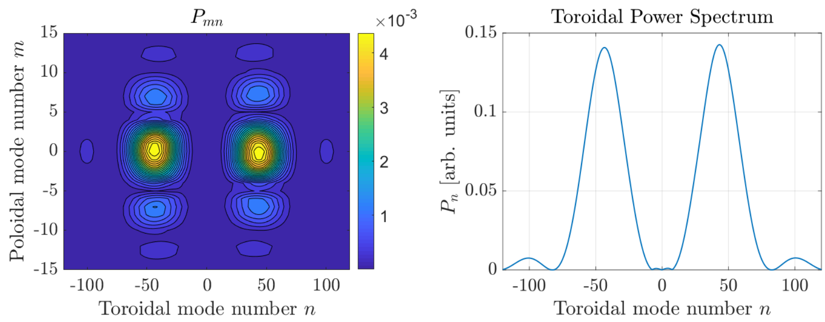

Figure 3: Two-dimensional power spectrum (left) and toroidal power spectrum (right).

the separatrix. This effect may come from the truncation of the tokamak. The Fourier basis functions are then no longer eigenfunctions of the system. Therefore, there may be coupling between the different modes. This problem can then be solved by modelling the complete tokamak.

Conclusion

An investigative study of a 3D model of ICRH in WEST has been conducted using the FEMIC code. A hot dielectric tensor was used in the plasma and a vacuum model in the SOL. The model had roughly 3.5 million degrees of freedom, requiring approximately 210 GB of RAM. However, at least 1 TB is needed to include a plasma model in the SOL, as well as using an appropriate mesh size and swept angle in the toroidal direction. A drawback of this model is that the dielectric tensor is evaluated for only one value of $k_{\parallel}$, despite the spectrum of parallel wave numbers, shown in Fig. 3. Future work includes determining the coupling impedance and adding a plasma model in the SOL.

References

[1] Heating ITER Physics Expert Group on Energetic Particles, Current Drive, and ITER Physics Basis Editors. Chapter 6: Plasma auxiliary heating and current drive. *Nuclear Fusion*, 39(12):2495, 1999.

[2] P. Vallejos et al. Effect of poloidal phasing on ICRH power absorption. *Nuclear Fusion*, apr 2019.

[3] M. Brambilla and R. Bilato. Simulation of ion cyclotron heating of tokamak plasmas using coupled Maxwell and quasilinear-Fokker–Planck solvers. *Nuclear Fusion*, 46(7):S387–S396, jun 2006.

[4] R.J. Dumont. Variational approach to radiofrequency waves in magnetic fusion devices. *Nuclear Fusion*, 49(7):075033, jul 2009.

[5] L. Villard et al. Global marginal stability of TAEs in the presence of fast ions. *Nuclear Fusion*, 35(10):1173–1190, oct 1995.

[6] S. Shiraiwa et al. HIS-TORIC: Extending core ICRF wave simulation to include realistic SOL plasmas. *Nuclear Fusion*, 57, 2017.

[7] P. Popovich et al. A full-wave solver of the Maxwell's equations in 3D cold plasmas. *Computer Physics Communications*, 175:250–263, 2006.

[8] D.G. Swanson. *Plasma Waves Second Edition*. IOP Publishing Ltd, 2003.

[9] P. Vallejos et al. A numerical tool based on FEM and wavelets to account for spatial dispersion in ICRH simulations. *Journal of Physics: Conference Series*, 1125:012020, nov 2018.